Title

Engineering Li/Na selectivity in 12-Crown-4–functionalized polymer membranes

Journal

Proceedings of the National Academy of Sciences of the United States of America, 118(37)

ISSN

0027-8424

Authors

Warnock, Samuel J
Sujanani, Rahul
Zofchak, Everett S
et al.

Publication Date

2021-09-14

DOI

10.1073/pnas.2022197118

Peer reviewed

Engineering Li/Na selectivity in 12-Crown-4–functionalized polymer membranes

Samuel J. Warnock[a,1], Rahul Sujanani[b,1], Everett S. Zofchak[b,1], Shou Zhao[c], Theodore J. Dilenschneider[b], Kalin G. Hanson[c], Sanjoy Mukherjee[d], Venkat Ganesan[b,2], Benny D. Freeman[b,2], Mahdi M. Abu-Omar[c,e,2], and Christopher M. Bates[a,c,d,e,2]

[a]Materials Department, University of California, Santa Barbara, CA 93106; [b]McKetta Department of Chemical Engineering, The University of Texas at Austin, Austin, TX 78712; [c]Department of Chemistry & Biochemistry, University of California, Santa Barbara, CA 93106; [d]Materials Research Laboratory, University of California, Santa Barbara, CA 93106; and [e]Department of Chemical Engineering, University of California, Santa Barbara, CA 93106

Edited by Howard A. Stone, Princeton University, Princeton, NJ, and approved April 1, 2021 (received for review December 5, 2020)

Lithium is widely used in contemporary energy applications, but its isolation from natural reserves is plagued by time-consuming and costly processes. While polymer membranes could, in principle, circumvent these challenges by efficiently extracting lithium from aqueous solutions, they usually exhibit poor ion-specific selectivity. Toward this end, we have incorporated host–guest interactions into a tunable polynorbornene network by copolymerizing 1) 12-crown-4 ligands to impart ion selectivity, 2) poly(ethylene oxide) side chains to control water content, and 3) a crosslinker to form robust solids at room temperature. Single salt transport measurements indicate these materials exhibit unprecedented reverse permeability selectivity (∼2.3) for LiCl over NaCl—the highest documented to date for a dense, water-swollen polymer. As demonstrated by molecular dynamics simulations, this behavior originates from the ability of 12-crown-4 to bind Na^+ ions more strongly than Li^+ in an aqueous environment, which reduces Na^+ mobility (relative to Li^+) and offsets the increase in Na^+ solubility due to binding with crown ethers. Under mixed salt conditions, 12-crown-4 functionalized membranes showed identical solubility selectivity relative to single salt conditions; however, the permeability and diffusivity selectivity of LiCl over NaCl decreased, presumably due to flux coupling. These results reveal insights for designing advanced membranes with solute-specific selectivity by utilizing host–guest interactions.

membranes | lithium | polymers | separation | selectivity

Lithium is a critical element in contemporary energy applications due to its pervasive use in electrochemical technologies (1–3). For example, lithium-ion batteries dominate the rechargeable market due to the light weight, large reduction potential, and high energy density of lithium (4, 5). Societal demand for lithium will continue to increase as mobile technology expands, especially with the imminent rise of electric vehicles (6–9). The majority of lithium is currently mined from pegmatite deposits and close-basined brines, with brines estimated to contain 58% of the world's identified lithium reserves (1, 10). Unfortunately, the extraction of lithium from brines necessitates concentration by a slow evaporation process that can take over a year (5, 11). An alternative source of lithium with concentrations comparable to brines (e.g., 100 to 1,000 mg/L) (12–14) is the vast volume of produced water (10.6 billion liters/day in the United States in 2017) generated from oil and gas operations (15), although lithium recovery from these wastewater streams is uncommon. The development of new, energy-efficient separation techniques with higher throughput would significantly decrease the cost of isolating lithium from traditional reserves as well as underutilized resources (11).

Polymeric membranes are an attractive alternative for aqueous lithium separation due to their energy efficiency and demonstrated scalability in various water purification processes (16). However, a key distinction in lithium recovery compared with water purification is the need for cation-specific selectivity due to the presence of multiple, concentrated cationic species in brines. Typical cationic contaminants in lithium-containing brines include Mg^{2+}, Na^+, K^+, and Ca^{2+}, with conventional lithium production often focusing on Mg^{2+} removal (6, 13). While monovalent/divalent separations have been successful over limited concentration ranges using conventional membranes (e.g., charged nanofiltration and ion exchange membranes) (11, 17–20), monovalent/monovalent (e.g., Li^+/Na^+) membrane separations, which would permit the selective removal of Li^+ from aqueous brines, remain difficult (21). Selectivity limitations between ions of the same valence arise from the fundamental physics governing ion transport through hydrated polymers (22). In swollen polymers devoid of significant polymer–solute-specific interactions, diffusivity selectivity typically depends on the solvated size of each solute in the membrane, with smaller hydrated species diffusing more quickly (23). For example, although the ionic radius of Li^+ is smaller than Na^+, its hydrated radius is larger (Li^+: 3.8 Å versus Na^+: 3.6 Å) due to a higher charge density (24), which leads to a diffusivity selectivity favoring Na^+ over Li^+ both in solution and in many hydrated polymers (23, 25). This typical trend in ion diffusivity may be reversed when ion dehydration effects or ion–pore-wall interactions become significant, most notably in metal organic frameworks and polymer systems containing subnanometer pores (26–29). However, such effects are uncommon in dense polymeric membranes, which are a cornerstone of desalination processes, and attempts to leverage

Significance

Lithium is a key ingredient in batteries, which are integral components of next-generation automobiles, airplanes, grid energy storage, and electronic devices. Unfortunately, lithium extraction from natural sources is laborious, slow, and costly, motivating the search for more efficient isolation techniques. While polymeric membranes could reduce the cost of lithium recovery, current membrane materials lack sufficient lithium-ion selectivity. To address this challenge, we introduce a class of polymeric membranes that incorporate ion binding sites, which significantly increases the transport selectivity of LiCl over NaCl. These studies provide guidelines and practical considerations for incorporating specific interactants into polymers that mediate selective ion transport.

Author contributions: S.J.W., R.S., E.S.Z., S.Z., T.J.D., V.G., B.D.F., M.M.A.-O., and C.M.B. designed research; S.J.W., R.S., E.S.Z., S.Z., T.J.D., K.G.H., and S.M. performed research; S.M. contributed new reagents/analytic tools; S.J.W., R.S., E.S.Z., S.Z., T.J.D., K.G.H., S.M., V.G., and C.M.B. analyzed data; and S.J.W., R.S., E.S.Z., V.G., and C.M.B. wrote the paper.

The authors declare no competing interest.

This article is a PNAS Direct Submission.

[1]S.J.W., R.S., and E.S.Z. contributed equally to this work.

[2]To whom correspondence may be addressed. Email: venkat@che.utexas.edu, freeman@che.utexas.edu, abuomar@chem.ucsb.edu, or cbates@ucsb.edu.

This article contains supporting information online at https://www.pnas.org/lookup/suppl/doi:10.1073/pnas.2022197118/-/DCSupplemental.

Published September 7, 2021.

specific interactions to promote ion–ion selectivity remain relatively unexplored.

In addition to diffusivity, differences in solubility can also influence selectivity. However, Na^+ and Li^+ often have limited solubility selectivity in polymers, leading to poor Li^+/Na^+ permeability selectivity (i.e., near or less than 1) (21, 22, 24). While some polymer materials can solubilize Li^+, such as poly(ethylene oxide)-based polymer electrolytes (30), or show limited solubility selectivity for Li^+ (poly(ethylene glycol) diacrylate hydrogels) (31), none have demonstrated substantial Li^+/Na^+ permeability selectivity, which could be useful for extracting lithium from brines. Overcoming this fundamental challenge requires new design concepts that favor the permeation of Li^+ over Na^+ (i.e., reverse selectivity).

One potential strategy to promote selective ion transport through polymeric membranes involves incorporating ligands to complex ions via host–guest interactions (6, 32–35). Crown ethers are a class of ligands known to bind various cations depending, in part, on the relative size of their cavity and the size of the target ion (35). For example, 12-crown-4 ether (12C4) forms reversible complexes with both Na^+ and Li^+ ions, where the relative affinity depends on the chemical environment (35–38). Some researchers have reported selective Li^+ transport by incorporating crown ethers into supported liquid membranes (34, 39, 40). However, these crown ethers are not chemically bound to the membrane and can leach into the surrounding solution. Other studies have grafted crown ethers onto polymers in an attempt to achieve cation-specific selectivity (32, 33, 41–43), but those studies focused primarily on equilibrium sorption properties rather than dynamic transport behavior; such materials would need to be operated in batch processes, which potentially requires more complex process design than continuous membrane filtration. Systematic investigations to elucidate the influence of water content and host–guest complexation on ion solubility and diffusivity would be a significant advancement. While these connections are highly complex, even for model systems (44), they would inform the design of selectivity in various applications (e.g., adsorption exchange, affinity chromatography, and membrane separations). Thus, there is a critical need to 1) develop novel polymer platforms that enable independent control over grafted-ligand chemistry and membrane water content, and 2) perform fundamental aqueous ion transport and selectivity studies in these systems.

Here, we report the sorption, transport, and selectivity properties of aqueous LiCl, NaCl, and $MgCl_2$ in dense, 12C4-functionalized membranes prepared using a tunable class of polynorbornene networks. The water content of these membranes can be modulated over a commercially relevant range (~10 to 50% by volume), and importantly, optimal compositions promote the selective transport of Li^+ over Na^+ and Mg^{2+} with permeability selectivities of 2.3 and 10, respectively, under single salt conditions. Molecular dynamics (MD) simulations indicate the origin of this unusual LiCl/NaCl transport selectivity is related to the selective binding of Na^+ to 12C4 and ion dehydration energies. We highlight the utility of a tight coupling between experiments and simulations to elucidate the fundamental impact of fixed 12C4 sites on concentration-gradient-driven ion transport in dense, hydrated polymers. Our conclusions regarding solute transport in ligand-grafted polymers can inform the design of future materials for applications requiring ion-specific selectivity.

Results and Discussion

Design and Synthesis of 12C4-Containing Membranes. The design of our 12C4-containing membranes utilizes three norbornene-based monomers that provide complementary functionality: 12C4 to introduce host–guest interactions, poly(ethylene oxide) (PEO) to control water uptake, and a crosslinker to form solids during in situ polymerization. Synthetic details for these monomers are provided in the *SI Appendix*, Scheme S1 and Figs. S1 and S2. Ring-opening metathesis polymerization (ROMP)—a versatile synthetic tool (45) with high reactivity and broad functional-group tolerance—was used to create membranes by solvent casting (Fig. 1). A dilute solution of the Grubbs third-generation catalyst was added to a prepolymerization mixture (*SI Appendix*, Table S1) containing monomers and solvent (dichloromethane, DCM). This mixture was quickly placed in a mold (*SI Appendix*, Fig. S3) and left under quiescent conditions for ~45 min while the DCM evaporated, followed by drying in vacuo. The resulting films were transparent (*SI Appendix*, Fig. S4), suggesting no phase separation or ordering on a length scale that would scatter visible light. The average composition of these 12C4-containing membranes—which is easy to control through the prepolymerization formulation—was verified by total-reflectance Fourier transform infrared spectroscopy and solid-state NMR spectroscopy (*SI Appendix*, Figs. S5 and S6). We emphasize that including 12C4 in these polynorbornene-based networks introduces an interaction not present in commercial membranes—complexation between monovalent cations and 12C4 (35)—which is fundamentally different from the steric and charge exclusion effects that typically govern ion permeation rates in membranes (22). This additional interaction imparts a potential pathway for selectivity between ions of the same valence, which commercial membranes are unable to achieve.

To ensure that 12C4 retains its ability to interact with monovalent cations when attached to a polynorbornene backbone, ^7Li NMR spectroscopy was used to determine the Li^+ binding constants for a norbornene-12C4 monomer and a representative polynorbornene homopolymer with pendant 12C4 moieties on each

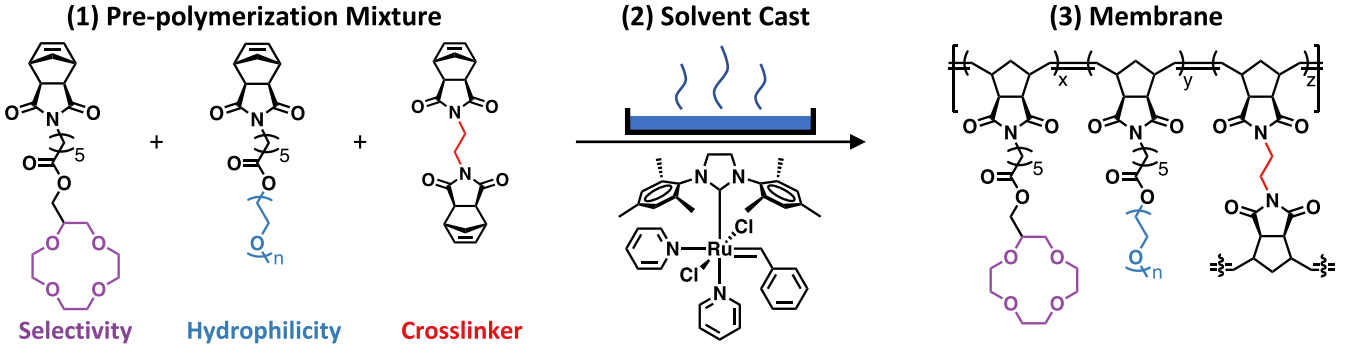

Fig. 1. Overview of the materials and solvent casting process used to create 12C4-containing polynorbornene membranes. Monomers (1) were dissolved in DCM at a known composition to prepare a prepolymerization mixture, followed by the addition of dilute G3 (a Ru-based catalyst). The mixture was quickly placed in a mold and left uncovered while most of the DCM evaporated (2). The final membrane was formed after drying in vacuo to ensure complete removal of the DCM (3).

repeat unit (*SI Appendix*, Figs. S7 and S8). These measurements were performed in acetone to ensure the 12C4-functionalized homopolymer was soluble, while practical Li^+ separations and our subsequent membrane characterization are performed under aqueous conditions. Solvent choice is well known to influence complexation (37, 38, 46), and thus these experiments do not reflect the binding constant in aqueous solutions or a hydrated membrane. Detailed procedures for binding-constant measurements are provided in the *SI Appendix*. In short, the binding constant showed little variation between the 12C4 monomer (log K_1 = 1.98) and 12C4-functionalized homopolymer (log K_1 = 1.77), suggesting that 12C4 retains its ability to complex cations when attached to a polynorbornene backbone.

Modulating Water Content with Membrane Composition. The permeability and selectivity of solutes through hydrated membranes is highly dependent on the equilibrium water content, as higher degrees of swelling tend to increase transport rates at the cost of selectivity (22, 23). Water content is often reported as a water uptake value, w_u (23, 47), in units of grams of water per gram of dry polymer:

$$w_u = \frac{m_{wet} - m_{dry}}{m_{dry}}, \quad [1]$$

where m_{wet} is the mass of the water equilibrated polymer, and m_{dry} is the mass of the dry polymer (23). Water content is also commonly expressed in terms of water volume fraction, ϕ_w, which may be calculated, assuming additivity, as follows:

$$\phi_w = \frac{w_u}{w_u + \rho_w/\rho_p}, \quad [2]$$

where ρ_w is the density of water (1 g/cm^3), and ρ_p is the density of the dry polymer (23). To control water content in our polynorbornene membranes, a hydrophilic norbornene-functionalized PEO macromonomer was incorporated at various loadings. The weight percent of crosslinker was kept constant, and the amounts of norbornene-functionalized 12C4 and PEO monomers were adjusted to vary the water content of different membranes. Water uptake and density measurements were performed for each membrane composition (*SI Appendix*, Table S2); water volume fractions are provided in Fig. 2. A linear trend is observed between water volume fraction and the weight percent of hydrophilic PEO monomer in the prepolymerization mixture. Varying the PEO macromonomer content from 0 to 10 weight (wt)% resulted in water contents ranging from 14 to 47% by volume, which is similar to the range of water contents in commercial membranes (23). Because solute transport models are often expressed in terms of ϕ_w (22), salt permeability and solubility measurements will be presented as a function of ϕ_w.

Membrane Transport Properties and LiCl/NaCl Selectivity. 12C4-functionalized polynorbornene membranes were characterized by measuring salt solubility (K_s) and permeability (P_s) (*SI Appendix*, Figs. S9–S11). Salt solubility describes the thermodynamic partitioning of a salt between an aqueous solution and a membrane as expressed by $K_s = C_m/C_s$, where C_m and C_s are the concentration of salt in the membrane (mol/L swollen polymer) and solution (mol/L), respectively (23). Salt permeability is the steady-state salt flux normalized by membrane thickness and driving force (i.e., a concentration gradient across the membrane) (23, 48). The solution-diffusion model relates these two properties and is the classical framework for interpreting solute transport through dense (i.e., nonporous) polymers (47, 49, 50). In this model, the salt permeability coefficient (P_s) is expressed as the product of the salt solubility coefficient (K_s) and the salt diffusion coefficient (D_s) (23, 47, 49, 50):

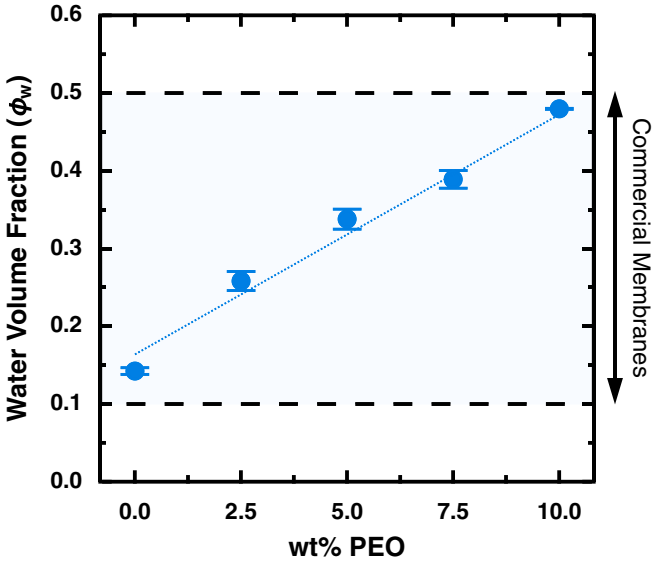

Fig. 2. Water volume fraction of polynorbornene membranes (filled blue circles) as a function of wt% PEO macromonomer in the prepolymerization mixture. The dashed black lines represent the range of water volume fractions (~0.1 to 0.5) typical of commercial membranes (23). Values and error bars represent the average and standard deviation of at least three separate samples.

$$P_s = K_s D_s. \quad [3]$$

Therefore, the salt permeability of a membrane can be modified by changes in the amount of salt that sorbs into the membrane or by changes in the salt diffusivity in the polymer matrix. The ability of a membrane to separate two species under a concentration gradient is often characterized by its permeability selectivity, which is the ratio of two species' permeabilities. Through the solution-diffusion model, permeability selectivity is comprised of two components—solubility selectivity and diffusivity selectivity. For LiCl/NaCl selectivity, these relationships are as follows:

$$\frac{P_{LiCl}}{P_{NaCl}} = \frac{K_{LiCl}}{K_{NaCl}} \frac{D_{LiCl}}{D_{NaCl}}, \quad [4]$$

where P_{LiCl}/P_{NaCl} is the permeability selectivity, K_{LiCl}/K_{NaCl} is the solubility selectivity, and D_{LiCl}/D_{NaCl} is the diffusivity selectivity.

To investigate the ion selective nature of the 12C4 membranes prepared in this study, salt solubility and permeability measurements were performed using aqueous LiCl, NaCl, and $MgCl_2$. The LiCl/NaCl pair is motivated by fundamental challenges that arise when separating ions of similar size and the same valence (21), while LiCl/$MgCl_2$ differentiation is of practical importance in current lithium production processes (6, 11). For each measurement, salt concentrations were held constant at 0.144 mol/L, corresponding to lithium concentrations relevant to natural brines and produced water (e.g., 1,000 mg/L) (6, 13). Single salt permeability through 12C4 membranes was measured and is reported as a function of water volume fraction (*SI Appendix*, Fig. S10). Generally, the permeability of each salt increases with water content, as expected from free volume and obstruction-based diffusion theories (51, 52). At low water volume fractions (e.g., 26 volume (vol)%), the order of permeation (i.e., NaCl > LiCl > $MgCl_2$) is the same as observed in aqueous solution (53). Remarkably, in 12C4 membranes prepared at intermediate water volume fractions (i.e., 34 to 39 vol%), LiCl permeates more quickly than NaCl. As water content further increases, the permeability of each salt becomes similar, but a slight preference for LiCl is maintained. Thus,

under single salt conditions, 12C4 membranes can exhibit an atypical reverse selectivity that favors the permeation of Li^+ over Na^+ as shown in Fig. 3*A*.

Salt solubility measurements (*SI Appendix*, Fig. S11) provide macroscopic insight into whether the permeation behavior exhibited by 12C4-functionalized polynorbornene membranes originates from partitioning (i.e., thermodynamic) effects or diffusivity (i.e., kinetic) effects. As expected, salt solubility generally increases with water volume fraction as the thermodynamic penalty for ions partitioning into the membrane is reduced. The solubility of $MgCl_2$ was consistently lower than the solubility of LiCl and NaCl, presumably due to a higher solvation energy for Mg^{2+} ions (54) that would increase the penalty for $MgCl_2$ to sorb into the membrane relative to other salts. In contrast to the permeability results, 12C4-functionalized polynorbornene membranes consistently showed higher solubility for NaCl than LiCl. This suggests that Na^+ exhibits stronger affinity for 12C4 groups than Li^+, which qualitatively agrees with binding-constant measurements in some solution-phase 12C4 systems in polar solvents (55).

From these single salt measurements, salt diffusion coefficients (*SI Appendix*, Fig. S12), along with LiCl/NaCl and LiCl/$MgCl_2$ permeability selectivity, solubility selectivity, and diffusivity selectivity were calculated for various water volume fractions as presented in Fig. 3. LiCl/NaCl permeability selectivity (Fig. 3*A*) follows an unusual, nonmonotonic trend with respect to water content, reaching a maximum value of ~2.3 at 34 vol% water. In terms of solubility selectivity, these membranes exhibit low LiCl/NaCl values (< 1), corresponding to selective partitioning of Na^+ over Li^+. As water volume fraction increases, LiCl/NaCl solubility selectivity increases and approaches 1. The LiCl/NaCl diffusivity selectivity was calculated via Eq. **4** and as shown in Fig. 3*A*, exceeds 1 and also follows a nonmonotonic trend with water content, reaching a maximum value of ~3.4 at 34 vol% water. The strong dependence of selectivity on water content suggests hydration plays a critical role in the selectivity mechanism of ligand-grafted membranes. Experimentally, the reverse LiCl/NaCl permeability selectivity observed at intermediate water content evidently originates from a diffusivity selectivity favoring LiCl over NaCl that dominates over an opposing trend in solubility selectivity favoring NaCl. As shown in Fig. 3*B*, these membranes also exhibit significant LiCl/$MgCl_2$ permeability selectivity (~10) at 26 vol% water that is primarily due to diffusivity selectivity. As water content increases, LiCl/$MgCl_2$ selectivity values are all near 1, suggesting that control of water content is important in designing monovalent/divalent selectivity. These results are qualitatively consistent with observations that the diffusivity of larger penetrants tends to be more sensitive to changes in free volume relative to smaller penetrants (23, 52).

To put these results into perspective, Fig. 4 compares the maximum LiCl/NaCl permeability selectivity of the 12C4-functionalized polynorbornene membranes prepared in this study with a number of conventional polymer membrane materials as a function of LiCl permeability, all under single salt conditions. In the absence of polymer–ion-specific interactions, most membranes exhibit $P_{LiCl}/P_{NaCl} < 1$ because the rate of ion permeation through hydrated polymers decreases with increasing solvated size (23, 24). To the best of our knowledge, the maximum LiCl/NaCl permeability selectivity observed in our 12C4-functionalized polynorbornene membranes (~2.3) is the highest to date for a dense, hydrated polymer under single salt conditions. This even exceeds the unusual Li^+/Na^+ selectivity recently observed in zeolitic imidazole frameworks (~1.4), which utilize Ångström-sized pores to sieve ions based on partially dehydrated radii (26). Li^+/Na^+ selectivity has also been observed in track-etched poly(ethylene terephthalate) membranes containing subnanometer pores due to ion-dehydration effects (27). The atypical LiCl/NaCl permeability selectivity reported here suggests that the incorporation of ligands (i.e., specific interactants) in hydrated polymers influences both solubility and diffusivity selectivity. This result indicates that host–guest interactions can be significant enough to reverse the transport selectivity of LiCl/NaCl in the bulk phase of a hydrated polymer.

Hydration Free Energy Controls 12C4 Binding. While salt solubility and permeability measurements are useful tools for macroscopically characterizing ion affinity and transport in polymers, information about the molecular interactions underlying these observations is still lacking (56–58). Understanding the molecular interactions between ligands, solutes, and water that govern selectivity is key to contextualizing experimental observations, as well as rationally

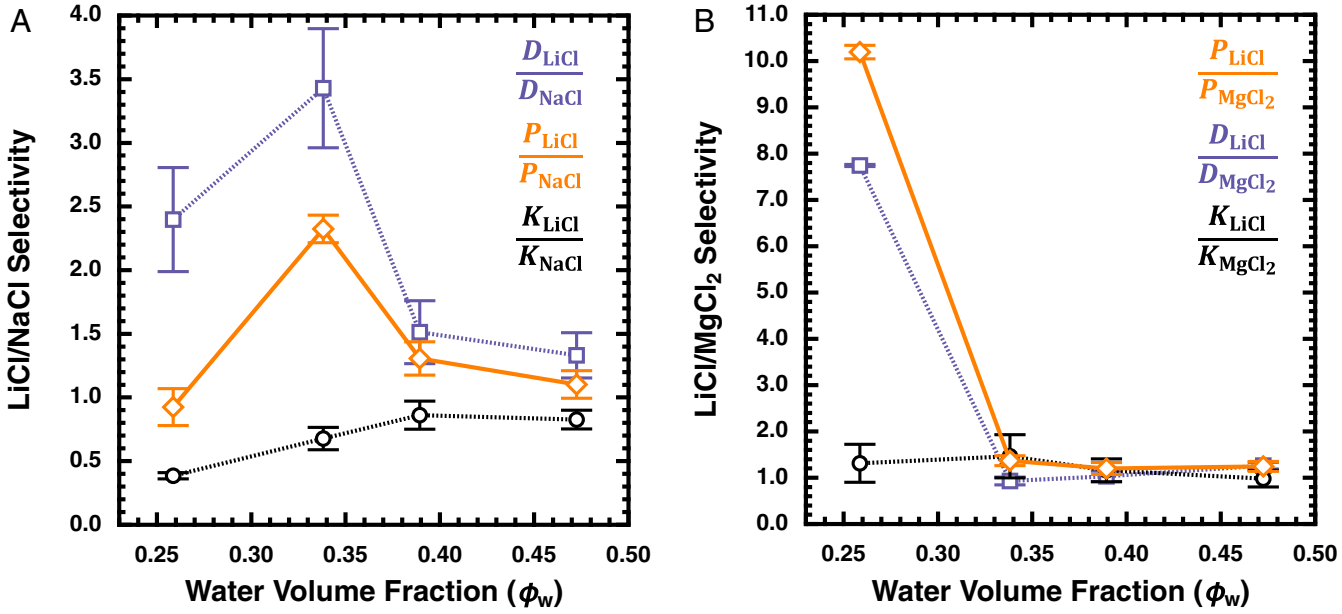

Fig. 3. Permeability selectivity (orange diamonds), solubility selectivity (black circles), and diffusivity selectivity (purple squares) of 12C4-functionalized polynorbornene membranes as a function of water volume fraction. (*A*) LiCl/NaCl selectivity. (*B*) LiCl/$MgCl_2$ selectivity. Values and error bars represent the average and standard deviation of at least three repeated measurements.

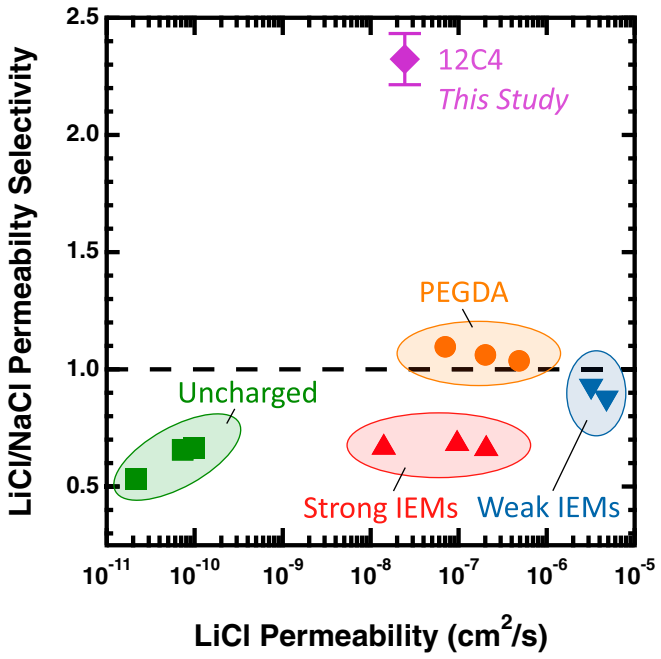

Fig. 4. Comparison of single salt LiCl/NaCl permeability selectivity among various polymer membranes as a function of LiCl permeability. IEM = ion exchange membrane, PEGDA = poly(ethylene glycol) diacrylate. Strong IEMs refer to materials containing charged groups that strongly dissociate (i.e., sulfonate and quaternary ammonium groups), while weak IEMs refer to materials containing charged groups that weakly dissociate (i.e., carboxylates). Our 12C4-containing polynorbornene membrane (5 wt% PEO, 34 vol% water) that showed the greatest LiCl/NaCl permeability selectivity is denoted with a purple diamond where the value and error bars represent the average and standard deviation from three repeated measurements. The dashed line denotes the boundary between Li^+-selective membranes (above) and Na^+-selective membranes (below). Adapted with permission from ref. 21.

designing selectivity in new membrane systems. To elucidate the origins of the LiCl/NaCl permeability selectivity observed in 12C4-functionalized membranes, atomistic MD simulations were performed for three types of systems: 1) aqueous salt solutions, 2) salt solutions containing 12C4, and 3) hydrated 12C4-functionalized polynorbornene membranes. Full details of the simulation methodology and parameters are provided in the *SI Appendix*, Fig. S13 and Tables S3–S8.

To quantify the interactions between monovalent cations and their environment, we computed the average number of water molecules and 12C4 oxygens coordinated with cations (*SI Appendix*, Figs. S14–S23). A complex between a crown ether and a cation (M^+) is typically depicted as the ion occupying the central cavity of the crown ether, which in the case of 12C4, corresponds to a cation coordinated with four oxygens (55, 59, 60). Another possibility is the formation of an $M(12C4)_2^+$ complex, where one ion is sandwiched between two 12C4s, corresponding to eight 12C4 oxygens coordinated with a single cation (60, 61). Fig. 5*A* shows the average coordination number between monovalent cations and 12C4 oxygens in an aqueous 12C4 salt solution and in a 12C4-functionalized polynorbornene membrane. For both the solution and the membrane, the average coordination number between Na^+ and 12C4 oxygens is greater than the average coordination number between Li^+ and 12C4 oxygens. The enhanced coordination between Na^+ and 12C4 oxygens is due to stronger interactions between 12C4 and Na^+ compared with 12C4 and Li^+, which is evidenced by significant differences in intensity of the first coordination shell in their respective pair correlation functions (*SI Appendix*, Figs. S14–S17). Transitioning from solution, where 12C4 is present as a small molecule, to the membrane case, where 12C4 is covalently bound to a polymer, both Li^+ and Na^+ exhibit a reduction in their average 12C4 oxygen coordination number. This may be due, in part, to the limited mobility or accessibility of 12C4 when chemically bound to a rigid polymer backbone. Interestingly, 12C4 transitions from forming predominantly $Na(12C4)_2^+$ complexes in aqueous solution to mostly $Na(12C4)^+$ complexes when tethered to the polymer chain (*SI Appendix*, Figs. S24–S27). Notably, the interactions between 12C4 and Li^+ are much weaker than those between Na^+ and 12C4, particularly in the membrane case where the average coordination number of Li^+ is near zero. That is, in the membrane, Li^+ does not exhibit any appreciable affinity for the 12C4 moieties.

Fig. 5*B* shows the coordination number between oxygen atoms from water molecules and Na^+ or Li^+ in two chemical environments: 1) salt solutions containing no 12C4, and 2) the 12C4-functionalized polynorbornene membrane. Our solution coordination results are in good agreement with previous experimental observations (62) and reported values for the ion and water models employed in this study (63). The presence of crown ethers significantly reduces the coordination between water oxygens and Na^+ due to the dehydration of Na^+ ions as they coordinate with 12C4. Although the reduction in Na^+ coordination with water oxygens is not as pronounced in the 12C4-functionalized polynorbornene membrane when compared with the 12C4 salt solutions (*SI Appendix*, Figs. S18–S23), it is still significant. In contrast, Li^+ shows little change in coordination with water in the 12C4 membrane system. Due to the higher charge density of Li^+ relative to Na^+ (64), there is a larger free energy penalty associated with displacing water molecules from the first coordination shell of Li^+, frustrating appreciable formation of $Li(12C4)_n^+$ complexes. Similar hydration free energy arguments have been used to justify 18-crown-6 ether selectivity favoring binding of K^+ over Na^+ in an aqueous environment (supported by potential of mean force calculations from MD simulations) (65). The observation of stronger interactions between 12C4 and Na^+ from our MD simulations is consistent with the experimental observation that $K_{LiCl}/K_{NaCl} < 1$, since these interactions would enhance partitioning of Na^+ into the membrane.

12C4 Coordination Reduces Diffusivity. The aforementioned experimental salt permeability and solubility measurements suggested that the observed LiCl/NaCl permeability selectivity results from a diffusivity selectivity favoring LiCl, which outweighs the solubility selectivity favoring NaCl. To confirm this experimental inference, cation self-diffusion coefficients in aqueous solution and a 12C4-functionalized polynorbornene membrane were calculated from linear fits to the long-time mean square displacement data computed from MD trajectories (*SI Appendix*, Table S9 and Figs. S28 and S29) (66). The self-diffusion coefficients for both ions decreased in the polymer matrix relative to the solution case, as expected, because the presence of polymer chains impedes ion transport, forcing both ions to traverse a more tortuous path (22, 47). Remarkably, the simulation data show that the diffusion coefficient of Li^+ is significantly larger than Na^+ in the membrane, as exemplified by a computed diffusivity selectivity $D_{Li}/D_{Na} \approx 9.5$. For comparison, in aqueous solution, $D_{Li}/D_{Na} \approx 0.8$ and 1.2 from experimental limiting conductivity data (53) and our simulations, respectively. Normalizing the diffusion coefficient in the membrane by the diffusion coefficient in solution reveals that this diffusivity selectivity is due to Na^+ transport being hindered more than Li^+ as a result of polymer-tethered 12C4. Li^+ diffusivity is reduced to ~6.3% of its bulk solution value in the membrane phase, while Na^+ diffusivity is reduced to about 0.8% of its bulk solution value (*SI Appendix*, Fig. S30). In the absence of solute-specific interactions, one would expect the relative decrease in diffusivity of both species to be approximately the same (51). This finding corroborates our experimental results and indicates that the observed reverse LiCl/NaCl diffusivity selectivity arises from strong, favorable interactions

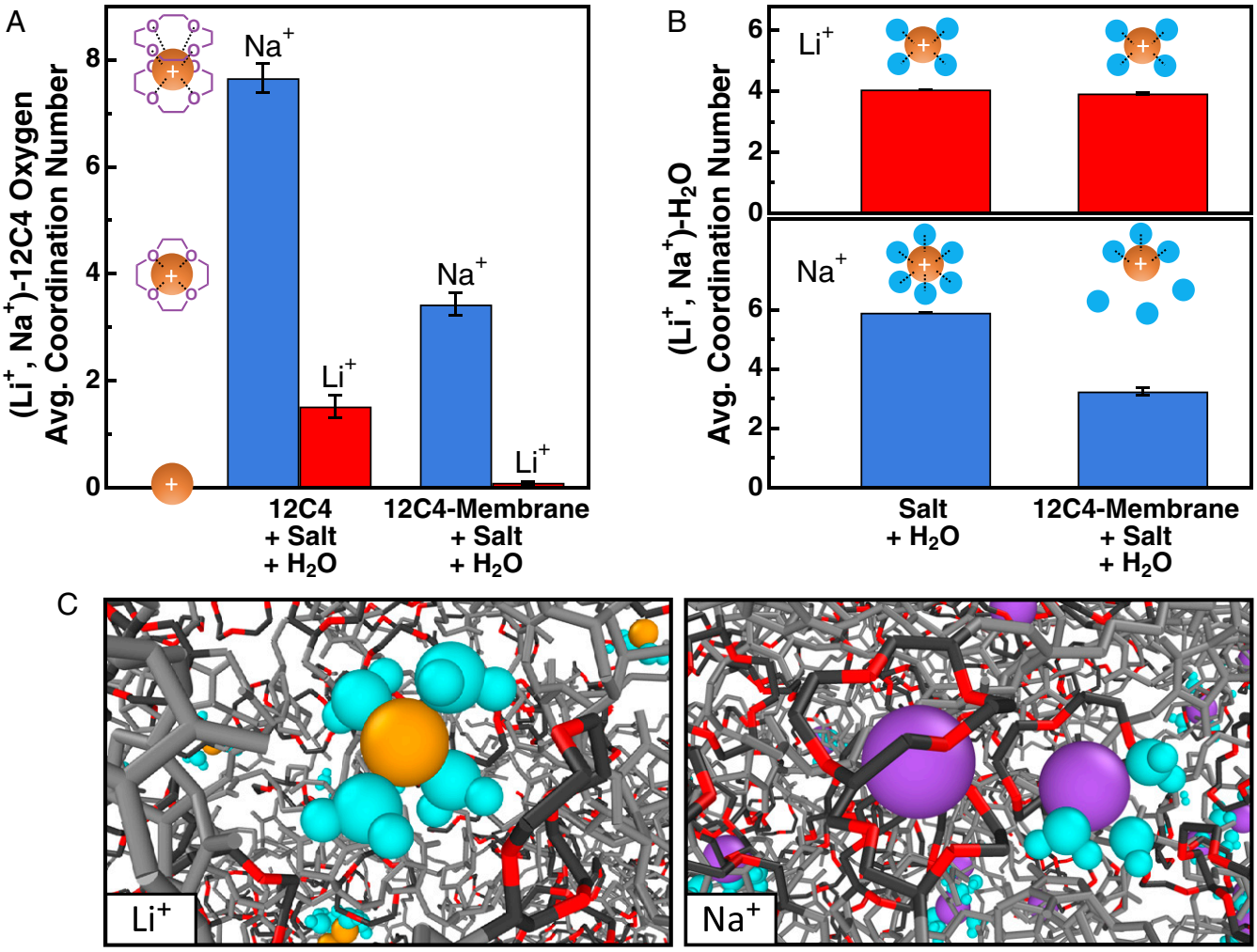

Fig. 5. Coordination behavior in aqueous solutions and 12C4-functionalized membranes as studied through MD simulations. (*A*) Average coordination number between Na^+ or Li^+ ions and 12C4 oxygens. 12C4 coordinates more readily with Na^+ than Li^+ in aqueous solutions and in hydrated polynorbornene membranes. (*B*) Average coordination number between water molecule oxygens and Li^+ or Na^+ in water (with no crown ethers) and in crown-ether–functionalized membranes. In the membrane, Li^+ maintains its first hydration shell while Na^+ partially dehydrates to complex with 12C4. (*C*) MD renderings of 12C4-based membranes highlighting (*Left*) a Li^+ ion (yellow) surrounded by its first hydration shell (cyan) and (*Right*) $Na(12C4)^+$ and $Na(12C4)_2^+$ complexes (Na^+ is purple). To improve visibility, 12C4 carbons and oxygens have been rendered black and red, respectively, while all other atoms in the polymer have been colored gray.

between Na^+ and 12C4, which impede the diffusion of Na^+ relative to Li^+.

Practical Considerations: Mixtures of Cations. While the LiCl/NaCl permeability selectivity observed under single salt conditions is remarkable, practical ion–ion separations require the removal of a relatively dilute ion from a concentrated mixture of other ionic species. Under these conditions, competitive sorption and flux coupling could influence selectivity in a nontrivial manner. To better understand the ion transport/selectivity of 12C4-functionalized membranes, we performed solubility and permeability measurements for an equimolar solution of LiCl and NaCl (0.072 mol/L of each) in the membrane composition that exhibited the highest LiCl/NaCl permeability selectivity under single salt conditions (5 wt% PEO). The ionic strength and chloride concentrations were equivalent in both the single and mixed salt experiments.

The solubility results (*SI Appendix*, Fig. S31) show that single salt solubility values and selectivities are maintained in the mixed salt case. These data are consistent with simulations which suggest there is no appreciable competition between Li^+ and Na^+ for 12C4 complexation (Fig. 5*A*). On the other hand, both the apparent permeability and diffusivity of LiCl and NaCl decreased and increased relative to their single salt values, respectively (*SI Appendix*, Fig. S31), leading to a reduced LiCl/NaCl permeability selectivity of 1.1. This result suggests the flux of each cation is coupled, with 12C4-complexed Na^+ sped up and noninteracting Li^+ slowed down relative to single salt conditions. Similar phenomena have been observed for ternary ion systems with a common anion in both aqueous electrolytes and reverse osmosis membranes (67, 68). Although P_{LiCl}/P_{NaCl} declined under mixed salt conditions, the apparent D_{LiCl}/D_{NaCl} was still much larger than unity (1.8), which represents a reversal from the typical order of diffusion in hydrated systems.

These observations are further rationalized using MD simulations (*SI Appendix*, Fig. S32). Here, the diffusivity of Cl^- is notably lower in the NaCl-equilibrated membrane than in the LiCl-equilibrated membrane because of electrostatic interactions between complexed Na^+ and Cl^-. In the mixed salt simulations, the presence of Li^+, which does not complex with 12C4, increases the diffusivity of Cl^- relative to the NaCl-equilibrated membrane,

presumably due to stronger electrostatic interactions between free Li^+ and Cl^- than complexed Na^+ and Cl^- (*SI Appendix*, Fig. S32*B*). The enhanced diffusivity of Cl^-, in turn, leads to a concomitant increase in Na^+ diffusivity relative to the NaCl-equilibrated membrane. Thus, the cation mobilities are indirectly linked to each other via their electrostatic interactions with Cl^-. This reduces Li^+ diffusivity and enhances Na^+ diffusivity in the mixed salt case relative to the respective single salt experiments.

Design Implications and Open Questions. The systematic study of ion transport/selectivity in 12C4 membranes outlined here provides general implications for the design of hydrated polymers grafted with ligands. In dense, hydrated polymers, host–guest interactions simultaneously enhance the solubility and reduce the diffusivity of an interacting solute, ultimately leading to an increased diffusivity selectivity favoring the noninteracting solute. With a fine balance of solubility and diffusivity selectivity, unusual permeability selectivity of the noninteracting solute can be achieved. However, practical limitations based on feed solutions biased in the undesirable solute and flux coupling of different ionic species present challenges for separation processes. Establishing whether the solubility/diffusivity trade-off for an interacting solute can be overcome requires detailed knowledge of the binding/dissociation kinetics for various membrane structures and ligand densities. Thus, it remains unknown if there are membrane properties that enhance the diffusion of an interacting solute such that its selective permeation can be achieved, or if such mechanisms are unattainable (29, 69). As an alternative material design approach to dense membranes that focuses on the selective transport of interacting solutes, functionalizing subnanometer pores with ligands could be a promising route to promote solute–solute selectivity (29, 70), provided only the complexing solute enters the pores without complete immobilization to the pore wall. Developing an understanding of separation performance under various driving forces (e.g., pressure- or electro-driven) and feed conditions in both dense and subnanometer porous membranes grafted with ligands would inform future materials design for specific applications.

Conclusions

In summary, we have introduced a polynorbornene-based membrane platform with tunable water content that is amenable to ligand functionalization (e.g., 12C4). Notably, at optimal water content, 12C4 moieties impart reverse permeability selectivity (~2.3) for LiCl over NaCl, which, to our knowledge, is higher than any previously reported value among hydrated polymers under single salt conditions. This behavior is ascribed to a combination of increased NaCl solubility and reduced NaCl diffusivity relative to LiCl due to the affinity of Na^+ with 12C4. MD simulations indicate these observations are rooted in the more facile dehydration of Na^+ compared to Li^+; the significant complexation of Na^+ with 12C4 impedes its diffusivity in the hydrated polymer. In contrast, Li^+ is relatively unperturbed by the presence of 12C4 in the membrane. Under mixed salt conditions, 12C4-functionalized membranes show identical K_{LiCl}/K_{NaCl} relative to single salt conditions; however, P_{LiCl}/P_{NaCl} and D_{LiCl}/D_{NaCl} are reduced by flux coupling. Together, our experimental and computational results provide fundamental insights into the transport properties of ions in polymeric membranes grafted with ion-selective ligands. These results hold significant design implications for ligand-grafted membranes in a range of applications requiring ion-specific selectivity, including membrane-based lithium recovery.

Materials and Methods

Full details regarding the synthesis of norbornene-functionalized monomers, ROMP polymerizations, material characterization, and simulation methodology are provided in the *SI Appendix*. All membranes were solution cast in a glove box. Gravimetric water uptake measurements were performed by equilibrating each membrane in deionized (DI) water, measuring the wet mass of the membrane, drying in vacuo, and recording its dry mass (Eq. **1**). Salt permeation experiments were performed by clamping a membrane between two chambers of a standard diffusion cell where the upstream (i.e., donor) side was filled with 35 mL 0.144 mol/L aqueous salt solution, and the downstream (i.e., receiver) side was initially filled with 35 mL DI water, with a stir bar added to each chamber. For single salt measurements, a conductivity probe was submerged in the receiving cell to track the flux of salt, and for mixed salt measurements, aliquots of known volume were sampled from the receiver chamber and analyzed using Flame Atomic Absorption to determine the flux of each cation. The opening of each chamber was covered to limit evaporation and exposure to air. Once steady state was reached, the permeation cell was disassembled and the thickness of the membrane was measured. Salt sorption experiments were performed by equilibrating membranes of known dimensions in a 0.144 mol/L salt solution. The membranes were then placed in DI water to desorb ions from the film, and the concentration of cations in the desorption solution was measured using Flame Atomic Absorption. All-atom MD simulations were performed using the Large-scale Atomic/Molecular Massively Parallel Simulator (LAMMPS) (71). We assumed that PEO does not contribute significant selective interactions with the ions and only served to modulate membrane water content. Thus, membrane systems were modeled as uncrosslinked 12C4-functionalized polynorbornene equilibrated in an aqueous salt solution. Water, polymer, and ions were modeled using the TIP4P/2005 (72), optimized potentials for liquid simulations (73–75), and Joung–Cheatham (~432 mM) force field parameterizations (76), respectively.

Data Availability. All study data are included in the article and/or *SI Appendix*.

ACKNOWLEDGMENTS. This work was supported as part of the Center for Materials for Water and Energy Systems (M-WET), an Energy Frontier Research Center funded by the US Department of Energy, Office of Science, Basic Energy Sciences under Award No. DE-SC0019272. The research reported here made use of shared facilities of the University of California, Santa Barbara Materials Research Science and Engineering Center (NSF DMR-1720256), a member of the Materials Research Facilities Network (https://www.mrfn.org/). The results in this paper were generated using high-performance computing resources provided by The University of Texas at Austin Texas Advanced Computing Center. This material is based upon work supported by the NSF Graduate Research Fellowship under Grant No. 000392968.

1. K. J. Schulz Jr, J. H. DeYoung, R. R. Seal, D. C. Bradley, *Critical Mineral Resources of the United States—Economic and Environmental Geology and Prospects for Future Supply* (U.S. Geological Survey, 2017) p. 797.
2. L. Li *et al*., Lithium recovery from aqueous resources and batteries: A brief review. *Johns. Matthey Technol. Rev.* **62**, 161–176 (2018).
3. B. Swain, Recovery and recycling of lithium: A review. *Separ. Purif. Tech.* **172**, 388–403 (2017).
4. N. Nitta, F. Wu, J. T. Lee, G. Yushin, Li-ion battery materials: Present and future. *Mater. Today* **18**, 252–264 (2015).
5. A. Manthiram, A reflection on lithium-ion battery cathode chemistry. *Nat. Commun.* **11**, 1550 (2020).
6. Y. Zhang, L. Wang, W. Sun, Y. Hu, H. Tang, Membrane technologies for Li^+/Mg^{2+} separation from salt-lake brines and seawater: A comprehensive review. *J. Ind. Eng. Chem.* **81**, 7–23 (2020).
7. J. F. Song, L. D. Nghiem, X.-M. Li, T. He, Lithium extraction from Chinese salt-lake brines: Opportunities, challenges, and future outlook. *Environ. Sci. Water Res. Technol.* **3**, 593–597 (2017).
8. B. Jaskula, 2017 minerals Yearbook - Lithium [advance release]. U.S. Geological Survey. (2020). https://prd-wret.s3.us-west-2.amazonaws.com/assets/palladium/production/atoms/files/myb1-2017-lithi.pdf. Accessed 28 September 2020.
9. G. Martin, L. Rentsch, M. Höck, M. Bertau, Lithium market research – global supply, future demand and price development. *Energy Storage Mater.* **6**, 171–179 (2017).
10. Y. Zhang, Y. Hu, L. Wang, W. Sun, Systematic review of lithium extraction from salt-lake brines via precipitation approaches. *Miner. Eng.* **139**, 105868 (2019).
11. X. Li *et al*., Membrane-based technologies for lithium recovery from water lithium resources: A review. *J. Membr. Sci.* **591**, 117317 (2019).
12. A. Kumar, H. Fukuda, T. A. Hatton, J. H. Lienhard, Lithium recovery from oil and gas produced water: A need for a growing energy industry. *ACS Energy Lett.* **4**, 1471–1474 (2019).
13. J. W. An *et al*., Recovery of lithium from Uyuni salar brine. *Hydrometallurgy* **117–118**, 64–70 (2012).
14. V. Flexer, C. F. Baspineiro, C. I. Galli, Lithium recovery from brines: A vital raw material for green energies with a potential environmental impact in its mining and processing. *Sci. Total Environ.* **639**, 1188–1204 (2018).

15. J. Veil, U.S. produced water volumes and management practices in 2017. Veil Environ. LLC (2020). www.veilenvironmental.com/publications/pw/pw_report_2017_final.pdf. Accessed 12 November 2020.
16. G. M. Geise *et al*., Water purification by membranes: The role of polymer science. *J. Polym. Sci., B, Polym. Phys.* **48**, 1685–1718 (2010).
17. G. Yang, H. Shi, W. Liu, W. Xing, N. Xu, Investigation of Mg^{2+}/Li^{+} separation by nanofiltration. *Chin. J. Chem. Eng.* **19**, 586–591 (2011).
18. C. H. Díaz Nieto *et al*., Membrane electrolysis for the removal of Mg^{2+} and Ca^{2+} from lithium rich brines. *Water Res.* **154**, 117–124 (2019).
19. S.-Y. Sun, L.-J. Cai, X.-Y. Nie, X. Song, J.-G. Yu, Separation of magnesium and lithium from brine using a Desal nanofiltration membrane. *J. Water Process Eng.* **7**, 210–217 (2015).
20. H. Wu *et al*., A novel nanofiltration membrane with [MimAP][Tf_2N] ionic liquid for utilization of lithium from brines with high Mg^{2+}/Li^{+} ratio. *J. Membr. Sci.* **603**, 117997 (2020).
21. R. Sujanani *et al*., Designing solute-tailored selectivity in membranes: Perspectives for water reuse and resource recovery. *ACS Macro Lett.* **9**, 1709–1717 (2020).
22. L. Masaro, X. X. Zhu, Physical models of diffusion for polymer solutions, gels and solids. *Prog. Polym. Sci.* **24**, 731–775 (1999).
23. G. M. Geise, D. R. Paul, B. D. Freeman, Fundamental water and salt transport properties of polymeric materials. *Prog. Polym. Sci.* **39**, 1–42 (2014).
24. E. R. Nightingale, Phenomenological theory of ion solvation. Effective radii of hydrated ions. *J. Phys. Chem.* **63**, 1381–1387 (1959).
25. Y. Liang *et al*., Polyamide nanofiltration membrane with highly uniform sub-nanometre pores for sub-1 Å precision separation. *Nat. Commun.* **11**, 2015 (2020).
26. H. Zhang *et al*., Ultrafast selective transport of alkali metal ions in metal organic frameworks with subnanometer pores. *Sci. Adv.* **4**, eaaq0066 (2018).
27. Q. Wen *et al*., Highly selective ionic transport through subnanometer pores in polymer films. *Adv. Funct. Mater.* **26**, 5796–5803 (2016).
28. X. Zhou *et al*., Intrapore energy barriers govern ion transport and selectivity of desalination membranes. *Sci. Adv.* **6**, eabd9045 (2020).
29. R. Epsztein, R. M. DuChanois, C. L. Ritt, A. Noy, M. Elimelech, Towards single-species selectivity of membranes with subnanometre pores. *Nat. Nanotechnol.* **15**, 426–436 (2020).
30. W. S. Loo, K. I. Mongcopa, D. A. Gribble, A. A. Faraone, N. P. Balsara, Investigating the effect of added salt on the chain dimensions of poly(ethylene oxide) through small-angle neutron scattering. *Macromolecules* **52**, 8724–8732 (2019).
31. E.-S. Jang *et al*., Influence of water content on alkali metal chloride transport in cross-linked Poly(ethylene glycol) Diacrylate.1. Ion sorption. *Polymer (Guildf.)* **178**, 121554 (2019).
32. A. Favre-Réguillon, N. Dumont, B. Dunjic, M. Lemaire, Polymeric and immobilized crown compounds, material for ion separation. *Tetrahedron* **53**, 1343–1360 (1997).
33. D. Sun *et al*., Fabrication of highly selective ion imprinted macroporous membranes with crown ether for targeted separation of lithium ion. *Separ. Purif. Tech.* **175**, 19–26 (2017).
34. H. Sakamoto, K. Kimura, M. Tanaka, T. Shono, Selective lithium ion transport through hollow-fiber membrane containing easily-dissociable 14-crown-4 derivative. *Bull. Chem. Soc. Jpn.* **62**, 3394–3396 (1989).
35. C. J. Pedersen, Cyclic polyethers and their complexes with metal salts. *J. Am. Chem. Soc.* **89**, 7017–7036 (1967).
36. H.-J. Buschmann, Stability constants and thermodynamic data for complexes of 12-crown-4 with alkali metal and alkaline-earth cations in methanol solutions. *J. Solution Chem.* **16**, 181–190 (1987).
37. A. D'Aprano, M. Salomon, V. Mauro, Solvent effects on complexation of crown ethers with $LiClO_4$, $NaClO_4$ and $KClO_4$ in methanol and acetonitrile. *J. Solution Chem.* **24**, 685–702 (1995).
38. A. J. Smetana, A. I. Popov, Lithium-7 nuclear magnetic resonance and calorimetric study of lithium crown complexes in various solvents. *J. Solution Chem.* **9**, 183–196 (1980).
39. R. M. Izatt *et al*., Proton-ionizable crown compounds: 5. Macrocycle-mediated proton-coupled transport of alkali metal cations in H_2O-CH_2Cl_2-H_2O liquid membrane systems. *J. Membr. Sci.* **31**, 1–13 (1987).
40. C. J. Hamilton, S. M. Murphy, B. J. Tighe, Synthetic hydrogels (10): Anomalous transport behaviour in crown ether-containing hydrogel membranes. *Polymer (Guildf.)* **41**, 3651–3658 (2000).
41. X. Luo *et al*., Lithium ion-imprinted polymers with hydrophilic PHEMA polymer brushes: The role of grafting density in anti-interference and anti-blockage in wastewater. *J. Colloid Interface Sci.* **492**, 146–156 (2017).
42. P. Wang, J. Dai, Y. Ma, L. Chen, J. Pan, Fabrication and evaluation of aminoethyl benzo-12-crown-4 functionalized polymer brushes adsorbents formed by surface-initiated ATRP based on macroporous polyHIPEs and postsynthetic modification. *Chem. Eng. J.* **380**, 122495 (2020).
43. J. Li *et al*., Preparation of crown-ether-functionalized polysulfone membrane by in situ surface grafting for selective adsorption and separation of Li^{+}. *ChemistrySelect* **5**, 3321–3329 (2020).
44. W. K. Kim, M. Kanduč, R. Roa, J. Dzubiella, Tuning the permeability of dense membranes by shaping nanoscale potentials. *Phys. Rev. Lett.* **122**, 108001 (2019).
45. C. Slugovc, The ring opening metathesis polymerisation toolbox. *Macromol. Rapid Commun.* **25**, 1283–1297 (2004).
46. Y. Gholiee, S. Salehzadeh, The solvent effect on selectivity of four well-known cryptands and crown ethers toward Na^{+} and K^{+} cations; a computational study. *J. Mol. Liq.* **309**, 113149 (2020).
47. H. Yasuda, C. E. Lamaze, L. D. Ikenberry, Permeability of solutes through hydrated polymer membranes. Part I. Diffusion of sodium chloride. *Macromol. Chem. Phys.* **118**, 19–35 (1968).
48. G. M. Geise, H. B. Park, A. C. Sagle, B. D. Freeman, J. E. McGrath, Water permeability and water/salt selectivity tradeoff in polymers for desalination. *J. Membr. Sci.* **369**, 130–138 (2011).
49. J. G. Wijmans, R. W. Baker, The solution-diffusion model: A review. *J. Membr. Sci.* **107**, 1–21 (1995).
50. G. M. Geise, B. D. Freeman, D. R. Paul, Characterization of a sulfonated pentablock copolymer for desalination applications. *Polymer (Guildf.)* **51**, 5815–5822 (2010).
51. J. S. Mackie, P. Meares, E. K. Rideal, The diffusion of electrolytes in a cation-exchange resin membrane I. Theoretical. *Proc. R Soc. London. Ser. A Math. Phys. Sci.* **232**, 498–509 (1955).
52. H. Yasuda, A. Peterlin, C. K. Colton, K. A. Smith, E. W. Merrill, Permeability of solutes through hydrated polymer membranes. Part III. Theoretical background for the selectivity of dialysis membranes. *Makromol. Chem.* **126**, 177–186 (1969).
53. R. A. Robinson, R. H. Stokes, *Electrolyte Solutions* (Dover Publications, Incorporated, Second Revised Edition, 2012).
54. Y. Marcus, Thermodynamics of solvation of ions. Part 5.—Gibbs free energy of hydration at 298.15 K. *J. Chem. Soc. Faraday Trans.* **87**, 2995–2999 (1991).
55. Y. Inoue, T. Hakushi, Y. Liu, L. H. Tong, Molecular design of crown ethers. 12. Complexation thermodynamics of 12- to 16-crown-4: Thermodynamic origin of high lithium selectivity of 14-crown-4. *J. Org. Chem.* **58**, 5411–5413 (1993).
56. D. R. Paul, The solution-diffusion model for swollen membranes. *Separ. Purif. Methods* **5**, 33–50 (1976).
57. M. A. Al-Obaidi, C. Kara-Zaitri, I. M. Mujtaba, Scope and limitations of the irreversible thermodynamics and the solution diffusion models for the separation of binary and multi-component systems in reverse osmosis process. *Comput. Chem. Eng.* **100**, 48–79 (2017).
58. P. Shao, R. Y. M. Huang, Polymeric membrane pervaporation. *J. Membr. Sci.* **287**, 162–179 (2007).
59. G. W. Gokel, D. M. Goli, C. Minganti, L. Echegoyen, Clarification of the hole-size cation-diameter relationship in crown ethers and a new method for determining calcium cation homogeneous equilibrium binding constants. *J. Am. Chem. Soc.* **105**, 6786–6788 (1983).
60. H. K. Frensdorff, Stability constants of cyclic polyether complexes with univalent cations. *J. Am. Chem. Soc.* **93**, 600–606 (1971).
61. R. E. C. Torrejos *et al*., Design of lithium selective crown ethers: Synthesis, extraction and theoretical binding studies. *Chem. Eng. J.* **326**, 921–933 (2017).
62. S. Varma, S. B. Rempe, Coordination numbers of alkali metal ions in aqueous solutions. *Biophys. Chem.* **124**, 192–199 (2006).
63. M. F. Döpke, O. A. Moultos, R. Hartkamp, On the transferability of ion parameters to the TIP4P/2005 water model using molecular dynamics simulations. *J. Chem. Phys.* **152**, 024501 (2020).
64. J. Mähler, I. Persson, A study of the hydration of the alkali metal ions in aqueous solution. *Inorg. Chem.* **51**, 425–438 (2012).
65. L. X. Dang, Mechanism and thermodynamics of ion selectivity in aqueous solutions of 18-crown-6 ether: A molecular dynamics study. *J. Am. Chem. Soc.* **117**, 6954–6960 (1995).
66. A. Einstein, Investigations on the theory of the Brownian movement. *Ann. Phys.* **17**, 549 (1905).
67. M. Soltanieh, S. Sahebdelfar, Interaction effects in multicomponent separation by reverse osmosis. *J. Membr. Sci.* **183**, 15–27 (2001).
68. H. K. Lonsdale, W. Pusch, A. Walch, Donnan-membrane effects in hyperfiltration of ternary systems. *J. Chem. Soc. Faraday Trans. 1 Phys. Chem. Condens. Phases* **71**, 501–514 (1975).
69. J. Kamcev, D. R. Paul, G. S. Manning, B. D. Freeman, Ion diffusion coefficients in ion exchange membranes: Significance of counterion condensation. *Macromolecules* **51**, 5519–5529 (2018).
70. A. Razmjou, M. Asadnia, E. Hosseini, A. Habibnejad Korayem, V. Chen, Design principles of ion selective nanostructured membranes for the extraction of lithium ions. *Nat. Commun.* **10**, 5793 (2019).
71. S. Plimpton, Fast parallel algorithms for short-range molecular dynamics. *J. Comput. Phys.* **117**, 1–19 (1995).
72. J. L. F. Abascal, C. Vega, A general purpose model for the condensed phases of water: TIP4P/2005. *J. Chem. Phys.* **123**, 234505 (2005).
73. W. L. Jorgensen, J. Tirado-Rives, Potential energy functions for atomic-level simulations of water and organic and biomolecular systems. *Proc. Natl. Acad. Sci. U.S.A.* **102**, 6665–6670 (2005).
74. W. L. Jorgensen, D. S. Maxwell, J. Tirado-Rives, Development and testing of the OPLS all-atom force field on conformational energetics and properties of organic liquids. *J. Am. Chem. Soc.* **118**, 11225–11236 (1996).
75. L. S. Dodda, I. Cabeza de Vaca, J. Tirado-Rives, W. L. Jorgensen, LigParGen web server: An automatic OPLS-AA parameter generator for organic ligands. *Nucleic Acids Res.* **45**, W331–W336 (2017).
76. I. S. Joung, T. E. Cheatham III, Determination of alkali and halide monovalent ion parameters for use in explicitly solvated biomolecular simulations. *J. Phys. Chem. B* **112**, 9020–9041 (2008).